Consequences of Molecular Bridging in Lamellae-Forming Triblock/Pentablock Copolymer Blends

Yoichiro Mori, Lisa S. Lim, and Frank S. Bates*

Department of Chemical Engineering and Materials Science, University of Minnesota, Minneapolis, Minnesota 55455

Received September 3, 2003; Revised Manuscript Received October 14, 2003

ABSTRACT: This study demonstrates that bridging (and possibly knotted looping) pentablock configurations in CEC/CECEC (triblock/pentablock) blends play significant roles in the shear-induced alignment and tensile mechanical properties of lamellae-forming block copolymers. Adding just 15 wt % pentablock to the triblock copolymer results in a perpendicular lamellar orientation at all applied strain amplitudes under reciprocating shear, similar to the behavior of the pure pentablock. In contrast, the triblock copolymer exhibits a transition from the perpendicular to the parallel orientation at high strain amplitudes. Approximately 10 wt % pentablock copolymer leads to a dramatic improvement in the strain at failure in shear aligned specimens when the strain is applied normal to the lamellae, a condition that results in brittle failure at small strains with the CEC triblock material. These findings are consistent with calculations that assume pentablock chains bridge the lamellae, thereby reinforcing the brittle C domains.

Introduction

Polystyrene-based block copolymers such as poly(styrene-*block*-butadiene-*block*-styrene) (SBS) have been exploited commercially for over three decades in footwear, in pressure-sensitive adhesives, in paving and roofing compounds, and as clear high-impact plastics.[1,2] These compounds combine the benefits of hard, glassy blocks and deformable, rubbery blocks into microphase-separated materials that exhibit properties ranging from low-modulus thermoplastic elastomers to tough plastics. Along with a host of beneficial properties, these materials suffer from several deficiencies including a modest upper use temperature established by the glass transition temperature of polystyrene (ca. 100 °C) and oxidative, thermal, and UV instabilities.[3]

Poly(cyclohexylethylene) (denoted PCHE or C)-based block copolymers diminish or eliminate most of these shortcomings without compromising essential properties.[4] PCHE, obtained by hydrogenating polystyrene (PS), has a glass transition temperature of about 147 °C, which is significantly higher than that of PS. Block copolymers formed from PCHE and saturated poly(diene) blocks (e.g., hydrogenated *cis*-1,4-poly(isoprene) and 1,4-poly(butadiene) known as poly(ethylenepropylene) (PEP) and poly(ethylene) (PE or E), respectively) are considerably more stable toward oxidative, thermal, and UV degradation relative to SBS.

Development of an efficient heterogeneous catalyst, comprised of an ultrawide-pore silica support decorated with platinum, has made commercial production of PCHE possible.[5] However, PCHE suffers from one important deficiency, a high entanglement molecular weight $M_{e,C} \approx 4 \times 10^4$ g/mol,[4] which results in a very brittle glassy plastic.

Combining PCHE with rubbery or semicrystalline polymers in the form of block copolymers is an attractive way to ameliorate the consequences of brittleness while retaining sample clarity and processability. A recent communication has shown that block architecture plays a key role in defining the ultimate physical properties.[6] Specifically, CEC triblock and CECEC pentablock copolymers respond differently when shear aligned specimens are strained along the lamellae normal. Whereas the triblock fails by brittle fracture at around 10% strain, the corresponding pentablock (similar composition and block molecular weights) yields and then is drawn to 270% strain before failing. These differences in solid-state mechanical properties are compounded by complex melt processing characteristics. Various combinations of shear rate, strain amplitude, and thermal history induce two distinct states of lamellae orientation. Here again CEC and CECEC behave very differently.[7]

These architecture-dependent differences have been attributed to the "stitching" of domains due to the existence of a C center block in CECEC pentablock copolymers.[6−8] Various molecular configurations for lamellae-forming AB diblock, ABA triblock, and ABABA pentablock copolymers are shown in Figure 1.[8] Diblock copolymers lack looping or bridging structures and are held together only through van der Waals interactions and chain entanglements. For ABA triblock copolymers, the B blocks will form bridges and loops (theory indicates about 40% bridges at equilibrium[9]), but the B blocks are unconstrained topologically. With ABABA pentablock copolymers, bridging and (knotted) looping structures occur in all domains. These differences in molecular architecture play an important role in microdomain alignment under flow and during solid-state mechanical deformation.

Flow-induced alignment of block copolymers has been studied for about 30 years;[2] lamellae and cylindrical morphologies are the most widely studied microstructures.[10−12] Lamellae are particularly interesting due to the clear distinction between three states: perpendicular, parallel, and transverse orientations. Koppi and coworkers[13] first reported a transition (denoted "flipping") between the perpendicular and parallel orientations using a reciprocating shear apparatus and poly(ethylethylene)−poly(ethylenepropylene) (PEE−PEP) diblock copolymers. This discovery sparked considerable inter-

* To whom correspondence should be addressed.

10.1021/ma035300q CCC: $25.00
Published on Web 11/26/2003

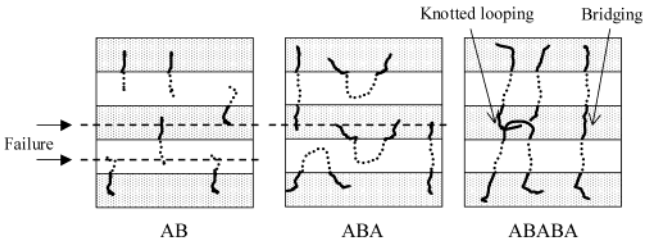

Figure 1. Molecular architecture of lamellae-forming AB diblock, ABA triblock, and ABABA pentablock copolymers. The dashed lines indicate fracture planes associated with domains containing unentangled blocks.

est in block copolymer melt dynamics.[2,7,8,10−21] Recently, Hermel and co-workers[7] investigated shear-induced alignment of nearly symmetric CEC and CECEC block copolymers, the same materials used to make blends in this study. CEC triblock copolymer formed purely parallel lamellae at very small strain amplitudes when sheared from the disordered state. Increasing the strain amplitude produced an abrupt transition to purely perpendicular lamellae, but the parallel orientation was reestablished at very large strain amplitudes. Conversely, CECEC pentablock copolymer formed only perpendicular lamellae at all strain amplitudes when sheared from the disordered state. These results for the CECEC pentablock copolymer are consistent with the findings of Vigild et al.[8] This work strengthens the idea that chain architecture plays an important role in determining the orientation of lamellae under shear.

Perhaps the most important block copolymer attributes are mechanical properties, which have been investigated extensively.[6,22−35] Most previous studies have focused on diblock[22−24] and triblock[24−33] copolymers, resulting in useful correlations between morphology and mechanical properties. Recently, higher order chain architectures, specifically pentablocks, have attracted attention.[6,34,35] Comparison of the deformation behavior of CEC triblock and CECEC pentablock copolymers containing a majority of glassy PCHE in thin film form was reported by Ryu and co-workers.[34] Both copolymers had the same molecular weight and weight fraction of PE in the form of cylinders. Using a micromechanical deformation technique, they found that the CECEC pentablock copolymer had surprisingly better resistance to crack formation compared to the CEC triblock copolymer. They attributed this difference to the presence of middle C blocks that bridged the cylindrical PE domains, which effectively prevent formations of voids and cracks in the C matrix. Hermel and co-workers[6,35] compared the tensile properties of macroscopic lamellae-forming CEC triblock and CECEC pentablock copolymers. When strained along the lamellae normal, CEC triblock copolymers failed in a brittle fashion while the CECEC pentablock copolymer yielded, necked, and strain hardened with ultimate failure at 270% strain. These two studies demonstrate that molecular architecture, in addition to morphology, is an important variable that influences block copolymer use properties.

This report describes melt flow and solid-state deformation experiments conducted with blends of CEC and CECEC block copolymers. These mixtures provide a continuously tunable degree of bridging (and possibly knotted looping) configurations. We have focused on the effect of pentablock content on shear-induced lamellae alignment and the associated macroscopic tensile mechanical properties. As described in the following sections, remarkably little CECEC polymer is required to achieve the qualitative effects found in the pure material.

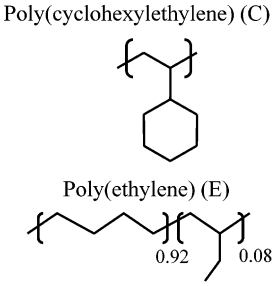

Figure 2. Chemical structure of the two polymers that make up the CEC triblock and CECEC pentablock copolymers.

Table 1. CEC Triblock and CECEC Pentablock Copolymers[a]

sample	M_n (g/mol)	M_w/M_n	mass fraction of C block
CEC	35 500	1.02	0.62
CECEC	54 400	1.03	0.57

[a] Molecular characterization data were provided by S.F. Hahn from the Dow Chemical Co.: M_n and M_w/M_n are based on size exclusion chromatography, and composition is based on ^{1}H NMR.

Experimental Section

Materials. Compositionally nearly symmetric lamellae-forming CEC triblock and CECEC pentablock copolymers were used in this study. C and E denote poly(cyclohexyl ethylene) and poly(ethylene), respectively (shown in Figure 2). Since the block copolymer molecular architecture is the focus of this work, all other factors including chemical compositions, weight fractions of the two components, and molecular weight per block were held nearly constant. Characterization results, taken from earlier publications,[6,7] are presented in Table 1. These polymers were produced by the Dow Chemical Co. by hydrogenating SBS and SBSBS precursor compounds using a heterogeneous porous silica supported platinum catalyst, where S and B refer to poly(styrene) and poly(butadiene), respectively.[5,7,36] The polybutadiene is a random copolymer containing 8% 1,2 and 92% 1,4 additions. Sequential anionic polymerization was employed in the production of the precursor compounds where the S blocks within each molecule are approximately equal in molecular weight; the B blocks in the pentablock are also equal in size. Greater than 99% saturation of the polymers was established using ^{1}H NMR. The mass fractions of C blocks are 0.62 for CEC and 0.57 for CECEC. Number-average molecular weights (M_n) are 35 500 g/mol for CEC and 54 400 g/mol for CECEC. The E blocks are a form of linear low-density poly(ethylene) with approximately 21 ethyl branches per 1000 backbone carbon atoms.[7,35]

Blending and Flat Sheet Sample Preparation. CEC/CECEC blends were prepared by codissolution in toluene at 90 °C followed by precipitation in methanol.[37] Blend samples were recovered and placed in a vacuum oven for about 24 h to remove residual solvent. Flat sheet specimens were compression-molded by pressing the precipitated powder between stainless steel plates separated by Teflon sheets. Pressure was applied stepwise, first to 1000 lb and then 2000 lb for 2 min each at 200 °C. The sample was then cooled to 100 °C for 2.5 min while holding the pressure. The samples were carefully removed from the molds at room temperature. Sample thickness was about 1 mm for shear alignment and 1.3 mm for rheology experiments.

Linear Viscoelastic Properties. Linear viscoelastic properties were measured using a Rheometrics ARES dynamic mechanical spectrometer. Here we restrict attention to isochronal (ω = 1 rad/s) dynamic storage modulus (G') measurements while heating or cooling at 2 °C/min. These experiments

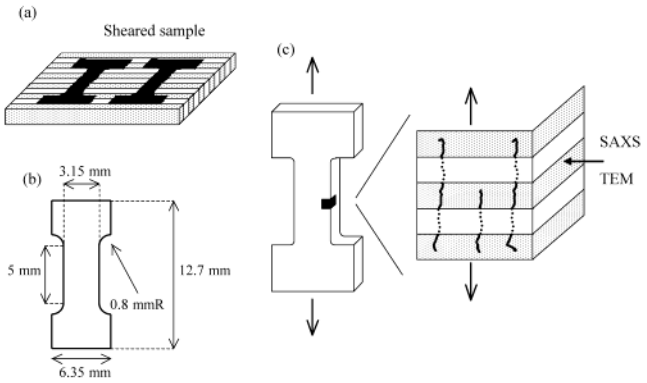

Figure 3. (a) Geometry of shear specimen shown with perpendicular lamellae (not drawn to scale) and tensile bar cutouts, (b) modified tensile bar dimensions, and (c) illustration of tensile test geometry and lamellae orientation.

were performed between 200 and 250 °C, which bracketed the order−disorder transition temperatures (T_{ODT}). This established procedure for determining T_{ODT} was described in earlier studies.[38−40]

Reciprocating Shear Machine. Samples were processed while under nitrogen using the reciprocating shear device described by Koppi[41] using channel-cut aluminum plates containing anodized rails. Specimens (1.5 cm × 1.9 cm × 1 mm) were placed between 2.54 cm × 1.91 cm aluminum plates placed 1 mm apart. Aluminum tape was used to cover the surfaces of the plates in order to allow for ease in sample removal. A single shear rate (0.48 s^{-1}) was employed for all experiments. Strain amplitude was varied from 0.5 to 5. Specimens were heated to T_{ODT} + 7 °C and held for 10 min at this temperature. Then, the shear device was turned on and the temperature was reduced at about 5 °C/min to T_{ODT} − 43 °C. Specimens were sheared isothermally at this temperature for 1 h, then the shear device was stopped, and specimens were cooled to room temperature over a 2 h period. This entire procedure is referred to as "shear from disorder".

Tensile Testing. Tensile stress ($\sigma = F/A_0$) was obtained as a function of applied strain ($\epsilon = \Delta l/l_0$) using a Rheometric MINIMAT instrument at room temperature. A modified tensile bar geometry was employed (Figure 3) due to the limited quantity of material available in each dynamically sheared sheet. Two tensile bars were cut from sheared specimens ($\dot{\gamma}$ = 0.48 s^{-1} and $\gamma = 1$) containing the perpendicular orientation (see Figure 3). These modified tensile bars had the following dimensions: gage length = 5 mm, gage width = 3.15 mm, fillet radius = 0.8 mm, overall length = 12.7 mm, and overall width = 6.35 mm. Tensile strains were applied along the lamellae normal as shown in Figure 3. Because of small variations in the applied force during the shear alignment process, the thickness varied somewhat between samples, although different specimens were uniformly thick and individually measured. At least five tensile experiments were conducted for each blend using a single crosshead speed of 10 mm/min. Hermel[35] has discussed the rate dependence to the stress−strain behavior for pure CEC and CECEC and evaluated differences between the ASTM standard test[42] (using standard type V bars) and the MINIMAT tensile tests using the modified bars. The modified tensile bars tend to fail prematurely relative to the ASTM specimens due to higher stress concentration caused by the smaller radius of curvature at the ends of the gage section. Nevertheless, to perform multiple tests on single sheets of aligned block copolymer, the smaller test geometry was employed. Although these measurements underestimate the true strain to failure, this systematic bias does not affect the general trends or adversely affect our conclusions regarding the role of the CECEC.

Small-Angle X-ray Scattering (SAXS). SAXS measurements were performed at the Institute of Technology Characterization Facility at the University of Minnesota. Copper Kα X-rays were generated by a Rigaku RU-200VBH rotating anode and focused using Franks mirror optics. Samples were contained in an evacuated chamber, and two-dimensional diffraction data were collected at room temperature. For shear orientation measurements the X-ray beam was directed normal to the plane of shear. The X-ray beam was directed normal to the plane defined by the strain and thickness directions of failed tensile specimens as indicated in Figure 3c.

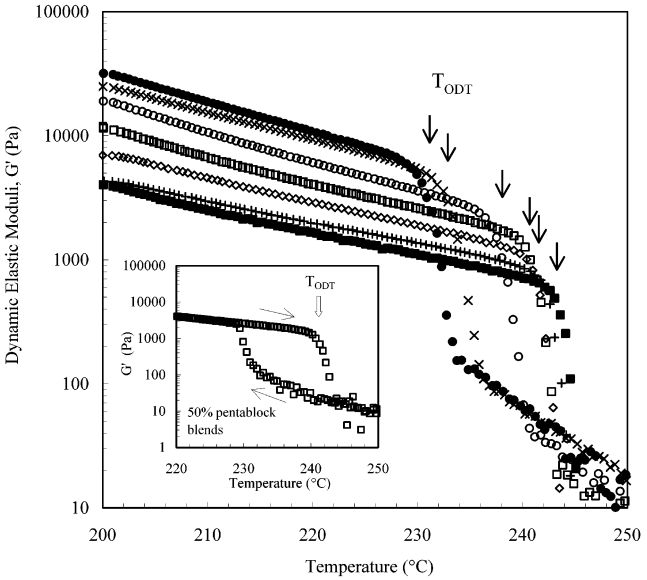

Figure 4. Temperature dependences of dynamic elastic modulus, G', measured while heating/cooling at 2 °C/min, with frequency $\omega = 1$ rad/s and shear strain $\gamma = 0.01$. (●) CECEC pentablock copolymer and blend samples with various wt % of pentablock: (×) 90, (○) 70, (□) 50, (◇) 30, (+) 10, and (■) pure CEC triblock copolymer.

Transmission Electrom Microscopy (TEM). TEM images were obtained from thin sections of block copolymer after staining with ruthenium tetraoxide following established procedures.[6] Sections were microtomed from the gauge portion of failed tensile specimens, thereby exposing the plane defined by the strain and thickness directions of the material as indicated in Figure 3c.

Results and Analysis

Order−Disorder Transition Temperature. The order−disorder transition temperature (T_{ODT}) plays a pivotal role in shear-induced alignment of block copolymers. Above T_{ODT} the material is in a disordered liquid state. Below T_{ODT} long-range translational order is established. T_{ODT} can be characterized by measuring the rheological response while heating and cooling samples between the ordered and the disordered states. Representative dynamic elastic modulus data, $G'(T)$, are plotted in Figure 4. Upon heating, G' drops abruptly at a temperature identified as T_{ODT}. Cooling leads to complete recovery of the elasticity as illustrated in the inset in Figure 4, although the hysteresis in $G'(T)$ evidences the first-order nature of this phase transition;[43] when cooled at 2 °C/min, the disordered material can be supercooled to approximately 15 °C below T_{ODT}. This widely reported behavior[8,38,44−46] can be attributed to a relatively low growth rate of the ordered state compared to the cooling rate. Conversely, the drop in G' during heating is much less rate dependent, particularly at slow heating rates[46] (≤2 °C/min), and we make use of these data to assign T_{ODT} as indicated by the arrows in Figure 4.

Figure 5 shows the relationship between T_{ODT} and the weight percent of CECEC pentablock in the CEC/

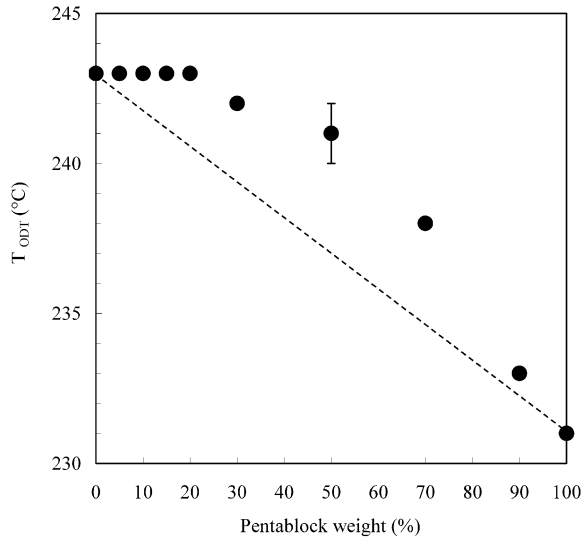

Figure 5. Relationship between T_{ODT} and CECEC concentration in triblock/pentablock blends. Each data point includes ±1 °C error due to instrument temperature resolution. T_{ODT} does not conform to a linear mixing rule for these CEC/CECEC blends.

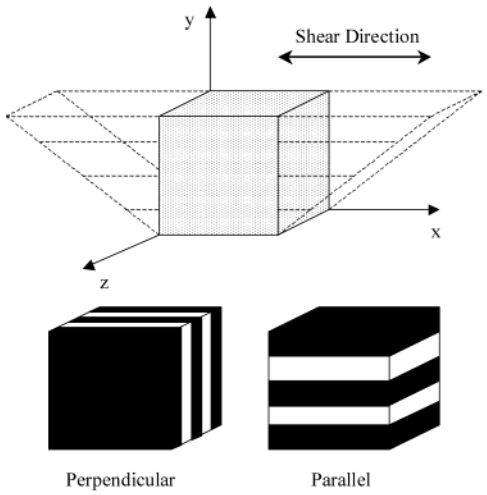

Figure 6. Illustration of coordinate system for reciprocating shear alignment and oriented lamellae. The axes identify the shear direction, *x*, the shear gradient direction, *y*, and the neutral direction, *z*. The parallel orientation has the lamellae normal aligned parallel to the shear gradient direction, *y*, and the perpendicular orientation has the lamellae normal aligned parallel to the neutral direction, *z*.

CECEC blends. The relationship is not linear. Although the difference in T_{ODT} for CEC and CECEC is not large (12 °C), the curvature in T_{ODT} (wt % CECEC) is well outside the relative experimental error. A similar nonlinearity has been reported by Gehlsen and co-workers[39] for blends of poly(ethylenepropylene)−poly(ethylethylene) (PEP−PEE) diblock and PEP−PEE−PEP triblock copolymers.

Shear-Induced Alignment. The effect of pentablock and strain amplitude on lamellae alignment was investigated while keeping shear rate, temperature relative to T_{ODT}, and the initial morphology of the specimen constant. Figure 6 illustrates the flow geometry and coordinate system employed, relative to the two states of alignment considered here; the axes identify the shear direction (*x*), the shear gradient direction (*y*), and the neutral direction (*z*). A parallel arrangement directs the lamellae normal along the shear gradient direction, *y*, while the perpendicular orientation places the lamellae normal parallel to the neutral direction, *z*.

Figures 7 and 8 show 2D-SAXS patterns obtained from sheared CECEC pentablock and CEC triblock copolymers obtained at two strain amplitudes, $\gamma = 1$ and 3. A pair of reflections along q_z in the q_x-q_z and q_y-q_z scattering planes and complete absence of scattering (except around the beam stop) in the q_x-q_y plane (Figure 7) are consistent with a perpendicular lamellae alignment for the pentablock copolymer at both strain amplitudes. In contrast, the CEC material exhibits scattering consistent with a perpendicular alignment at $\gamma = 1$ but a parallel alignment at $\gamma = 3$. This transition is most efficiently illustrated with the X-ray beam directed along the shear (*x*) axis where the reflections are evident in both orientations, rotated by 90°.

Representative SAXS data (q_y-q_z plane) obtained from CECEC/CEC blends ($\gamma = 3$) are presented in Figure 9. Clear evidence of a perpendicular alignment is found down to 15% CECEC. At 10% pentablock the peak intensity rotates into q_y; reduction to 5% and 0% (Figure 8) CECEC enhances the anisotropy in the scattering indicative of a more coherent parallel orientation.

Figure 10 summarizes all our shear alignment results. The pentablock copolymer has greatest impact on the shear alignment process at larger strain amplitudes. Remarkably, just 15 wt % CECEC induces the same state of orientation found in the pure pentablock material. At strain amplitudes $\gamma \leq 2$ it is possible to produce the perpendicular arrangement over the complete range of blend compositions, a feature that is exploited in the next section.

Notwithstanding the profound influence of strain amplitude and pentablock content on domain orientation, these parameters have no perceptible effect on the domain periodicity, obtained from the principal SAXS reflections, $d^* = 2\pi/q^*$. Table 2 shows the lamellae periodicity at $\gamma = 0.5$ and 3. These data show that all samples have a periodicity of 17−18 nm.

Mechanical Properties. Reciprocating shear permits formation of highly ordered lamellae with a perpendicular or parallel orientation. Here we take advantage of a single orientation, perpendicular lamellae obtained with $\gamma = 1$, in exploring the consequences of pentablock content on mechanical properties during tensile deformation. We chose to apply a tensile strain normal to the plane of the lamellae since the CEC and CECEC mechanical properties differ most dramatically in this configuration.[6] This geometry is easily accessed with the perpendicular alignment as illustrated in Figure 3a.

Figure 11 displays representative stress−strain curves obtained as a function of pentablock content in CECEC/CEC blends. Each figure contains at least five separate traces recorded while loading the specimens in tension. With the exception of panel d (10% CECEC) and panel e (5% CECEC) the traces cluster around a common response with well-defined strains at failure where sample fracture is identified by the symbol "×".

The undiluted CECEC pentablock copolymer (Figure 11a) exhibits three distinct deformation zones:[6] elastic ($0 \leq \epsilon \leq 0.15$), necking ($0.2 \leq \epsilon \leq 1.3$), and strain hardening ($1.3 \leq \epsilon \leq 2.7$). Yielding and drawing are accompanied by a significant reduction in thickness ($\Delta t/t_0 = 0.31$ at failure) with little change in width ($\Delta w/w_0$

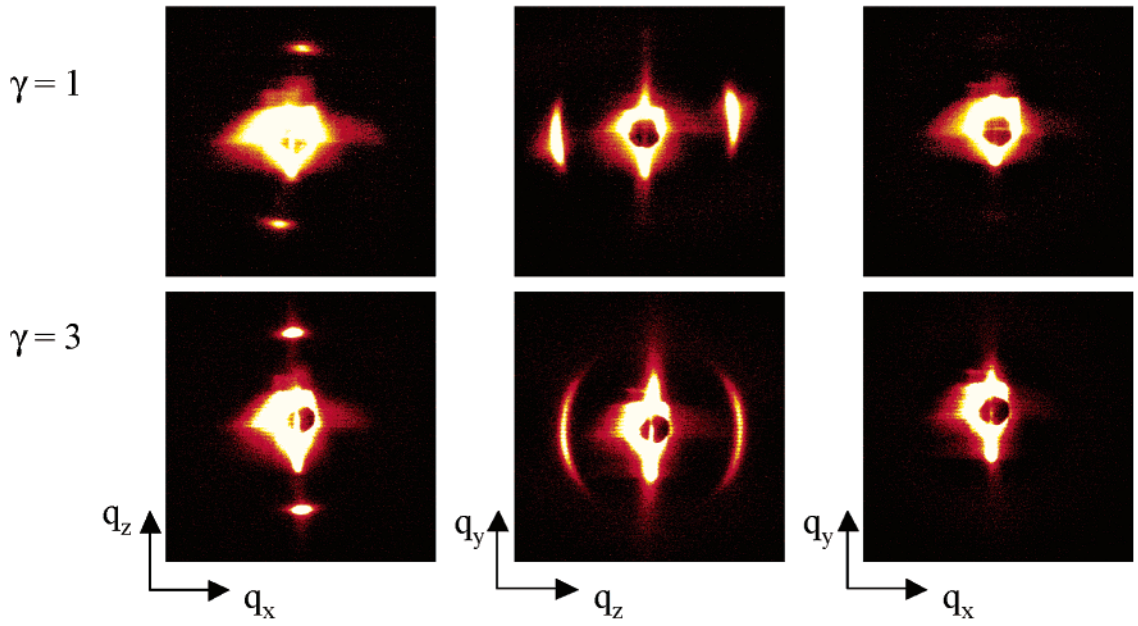

Figure 7. SAXS patterns obtained from CECEC pentablock copolymer after shear alignment with two strain amplitudes. Figure 6 identified the coordinate system. These scattering patterns are consistent with perpendicular lamellae orientation at both amplitudes.

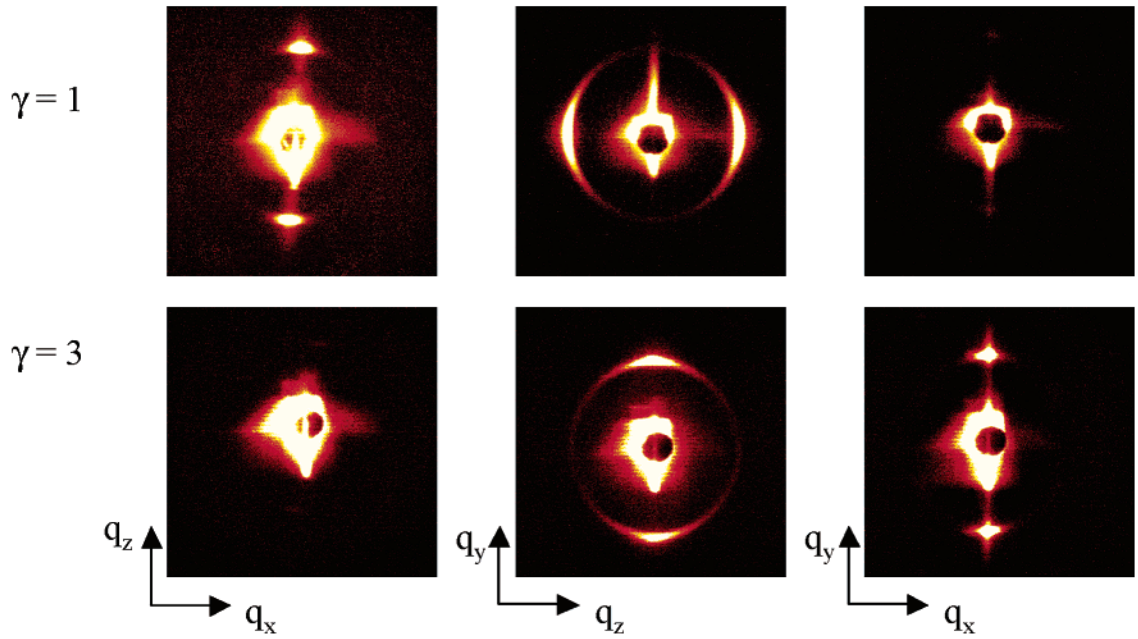

Figure 8. SAXS patterns obtained from CEC triblock copolymer after shear alignment with two strain amplitudes. These patterns are consistent with perpendicular lamellae orientation at $\gamma = 1$ and parallel lamellae at $\gamma = 3$.

= 0.04 at failure). In contrast the CEC triblock copolymer displays brittle behavior with an average strain at failure of $\langle\epsilon_f\rangle \approx 0.15$, somewhat higher than what we reported earlier;[6] we do not understand the origin of this minor difference although we suspect it may reflect subtle variations in the quality of lamellae alignment due to processing differences (see below). Blend samples containing as little as 20% pentablock (Figure 11c) behave like the pure CECEC material; the principal consequence of adding triblock copolymer is a reduction in the average strain at failure from 270% to about 200%. At and below 15% CECEC the blends behave erratically as shown in Figure 11d,e. Anisotropic necking in all the blended specimens resembles the pure pentablock result ($\Delta t/t_0 = 0.25$ and $\Delta w/w_0 = 0.03-0.05$).

A summary of the strain at failure for all our experiments is provided in Figure 12. As the CECEC content is reduced from 100% to 20%, the strain at failure values cluster around a line that decreases by about 30% in $\langle\epsilon_f\rangle$. From 15% to 5% ϵ_f fluctuates between the tough and brittle limits set by the 20% and 0% (i.e., pure triblock) materials, respectively. Presumably, ϵ_f is sensitive to factors other than the intrinsic strength of the material in the limit of low CECEC loading, such as surface and bulk imperfections, which likely facilitate crack formation in an unpredictable manner.

Although the stress−strain curves in Figure 11a−c are quite similar, the samples exhibit distinctly different optical properties when strained. Photographs of representative failed tensile bars (corresponding to the

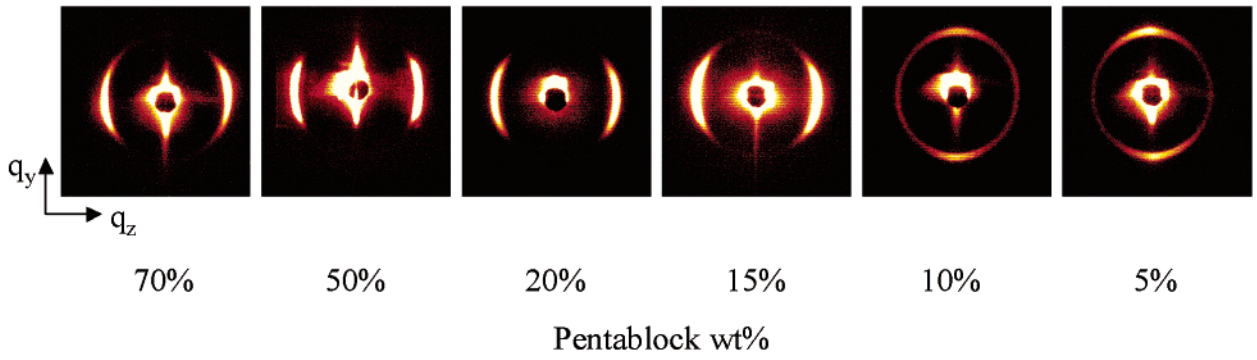

Figure 9. SAXS patterns obtained from CECEC/CEC blends dynamically sheared with strain amplitude $\gamma = 3$. These images were obtained with the X-ray beam directed along the shear direction (see Figure 6). At and above 15 wt % pentablock copolymer a perpendicular lamellae arrangement is indicated while lower concentrations result in a parallel orientation.

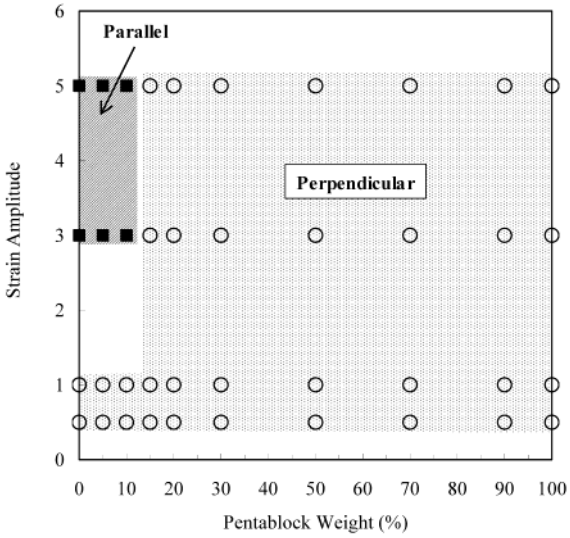

Figure 10. Lamellae orientation map for CECEC/CEC blends as a function of pentablock concentration and strain amplitude, where ○ and ■ indicate perpendicular and parallel orientations, respectively. Each specimen was sheared while cooling from the disordered state at a shear rate = 0.48 s^{-1}.

Table 2. Lamellae Periodicity

	lamellae periodicity d^* (nm)	
samples	at $\gamma = 0.5$	at $\gamma = 3.0$
CECEC pentablock	17.2	17.2
pentablock 90%	16.9	17.0
pentablock 70%	16.9	17.1
pentablock 50%	17.3	17.2
pentablock 30%	17.3	17.3
pentablock 20%	17.3	17.6
pentablock 15%	17.4	17.6
pentablock 10%	17.6	17.0
pentablock 5%	17.7	17.3
CEC triblock	17.7	17.2

filled symbols in Figure 12) are shown in Figure 13. During stretching and after failure the CECEC pentablock copolymer remains relatively transparent, noticeably more so than reported in an earlier publication;[24] note that most of the strain is not recovered upon failure. As the CECEC content decreases, yielding, necking, and drawing are accompanied by significant strain whitening which persists in the broken tensile bars as is evident in the photographs of the 50% and 20% specimens. The failed CEC specimen is optically transparent. Two broken 10% CECEC specimens are shown in Figure 13b, one that failed at $\epsilon = 40\%$ and another at $\epsilon = 170\%$. Both exhibit intense strain

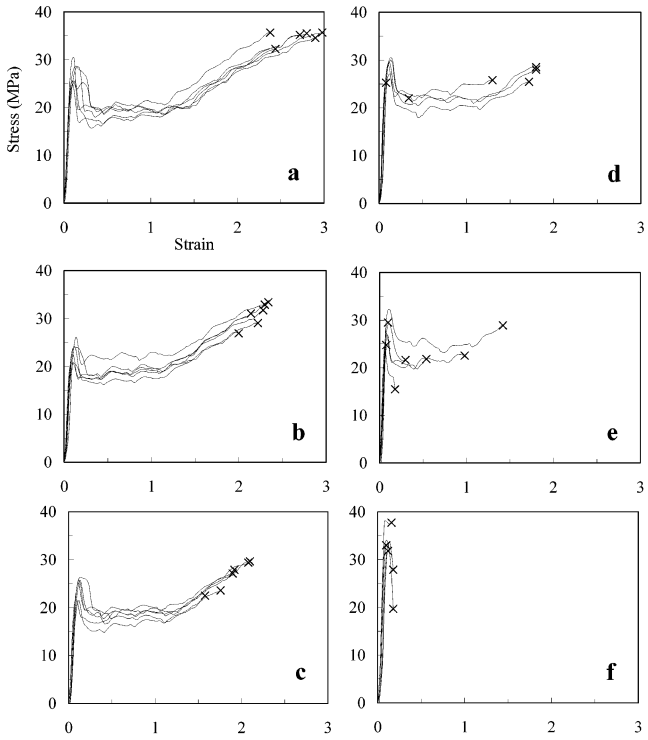

Figure 11. Tensile properties of sheared (a) CECEC pentablock, (b) blend sample with 50% of pentablock, (c) blend sample with 20% of pentablock, (d) blend sample with 10% of pentablock (e), blend sample with 5% of pentablock, and (f) CEC triblock when loaded along the lamellar normal at crosshead speed of 10 mm/min. Failure points are shown as "×".

whitening, the former around the crack and the latter throughout the strained gage section.

SAXS patterns obtained from the necked (and whitened) region of four of the broken samples shown in Figure 13 (100%, 50%, 20%, and 10% CECEC) are illustrated in Figure 14; the X-ray beam was directed normal to the thickness direction (see sketch). In each case a set of four distinctive reflections are seen consistent with the results reported earlier by Hermel et al.[6] for perpendicularly oriented pentablock strained normal to the lamellae. Curiously, the 100% pentablock SAXS pattern is nearly devoid of low-q scattering (around the beamstop), in contrast with the previous result[6] obtained from the same material, prepared under similar (but not identical) conditions. We address this apparent contradiction in the next section. Forward scattering around the beamstop increases dramatically

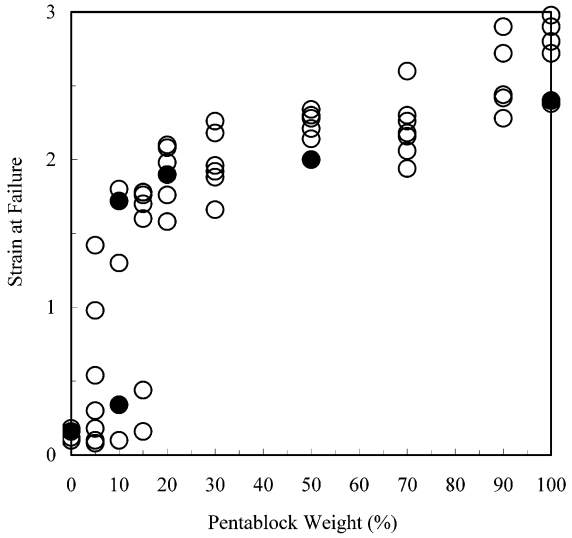

Figure 12. Relationship between strain at failure and weight percent pentablock in CECEC/CEC blends. Filled symbols identify broken specimens that were photographed and are presented in Figure 13.

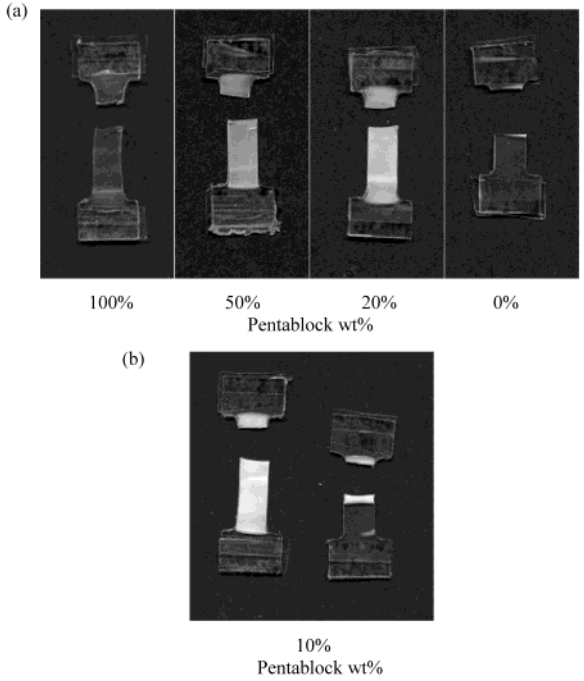

Figure 13. Photographs of representative failed tensile bars. (a) CECEC/CEC blend samples with indicated percentage of pentablock copolymer. (b) Blend sample containing 10% pentablock. As the amount of pentablock decreases, the level of strain whitening increases, suggestive of extensive cavitation.

as the pentablock content is reduced, coincident with the development of strain whitening (Figure 13).

Representative TEM images obtained from thin sections taken from the failed pentablock and 10% CECEC blend specimens (shown in Figure 13) are presented in Figures 15 and 16, respectively. These pictures reveal extensive lamellae buckling, consistent with an earlier report for the pure pentablock and in agreement with the SAXS results (Figure 14). The lower magnification images reveal bands of tilted lamellae, roughly 200−300 nm wide, arranged in a chevron pattern with an alternating angle of approximately 65°. Other than buckled lamellae the pure pentablock morphology is remarkably free of defects. In contrast, the 10% CECEC blend micrographs contain clear evidence of void formation with holes ranging in size from less than 100 nm to as much as 400 nm in diameter. We associate these cavitations with the opacity found in Figure 13b.

Discussion

Remarkably little pentablock copolymer is required to access the benefits of bridging and possibly knotted looping configurations in blends with triblock copolymer. Based on Figures 10 and 12, the threshold level is about 10−15% pentablock copolymer. What distinguishes CECEC from CEC is the center C block, which can form bridges or topologically constrained (knotted) looping configurations (see Figure 1), thereby stitching together all C (and E) domains. We have two reasons to believe that bridging is the predominant factor.

First, to be effective two looping center C blocks must knot by topological entanglement from opposite sides of a C domain. This process will be second order in pentablock concentration; hence, we expect the physical consequences (e.g., enhanced toughness) to depend on the square of the pentablock concentration. A 10% pentablock threshold seems unlikely on the basis of this mechanism since relatively few center blocks would be topologically paired. However, the weak concentration dependence to ϵ_f (Figure 12) between 100% and 20% CECEC may reflect the loss of knotted looping configurations.

Second, we can estimate the number of bridging blocks required to enhance the strength of the brittle C domains so that yielding in the E domains becomes the limiting factor. This estimate agrees with the transition region in Figure 12 as detailed below.

All the C blocks in CEC and CECEC are well below the entanglement molecular weight,[4] $M_{e,C} = 4 \times 10^4$ g/mol. Therefore, we assume that brittle failure in oriented CEC, when strained normal to the lamellae, reflects fracture of C domains due to facile chain pull out. Analogous failure of CECEC requires cleavage of center C blocks or yielding of the E domain material, which can be estimated as $\sigma_Y \approx 25-30$ MPa (see Figure 11). Assuming the contributions due to bridging and looping center C blocks are additive, the criterion for yielding becomes

$$\sigma_{\text{bridging}} + \sigma_{\text{knotted looping}} > \sigma_Y \qquad (1)$$

For reasons already discussed $\sigma_{\text{knotted looping}}$ will be neglected since we are primarily interested in the low pentablock concentration limit. The cross-sectional area of a bridging C block, A, can be calculated from the molecular weight M_C and density ρ

$$A = \frac{M_C}{N_A \rho d} \qquad (2)$$

where N_A is Avogadro's number and d is the thickness of the C domains. Since the lamellae periodicity is about 18 nm (Table 2), d is approximately 9 nm. On the basis of an overall pentablock molecular weight of 54 400 g/mol and a C block mass fraction of 0.57 split evenly between each of three blocks, M_C is approximately 10 250 g/mol. For a C density of 0.947 g/cm^3,[5] A is calculated to be 2.0×10^{-18} m^2.

Creton and co-workers[47] investigated failure mechanisms of polymer interfaces between polystyrene and

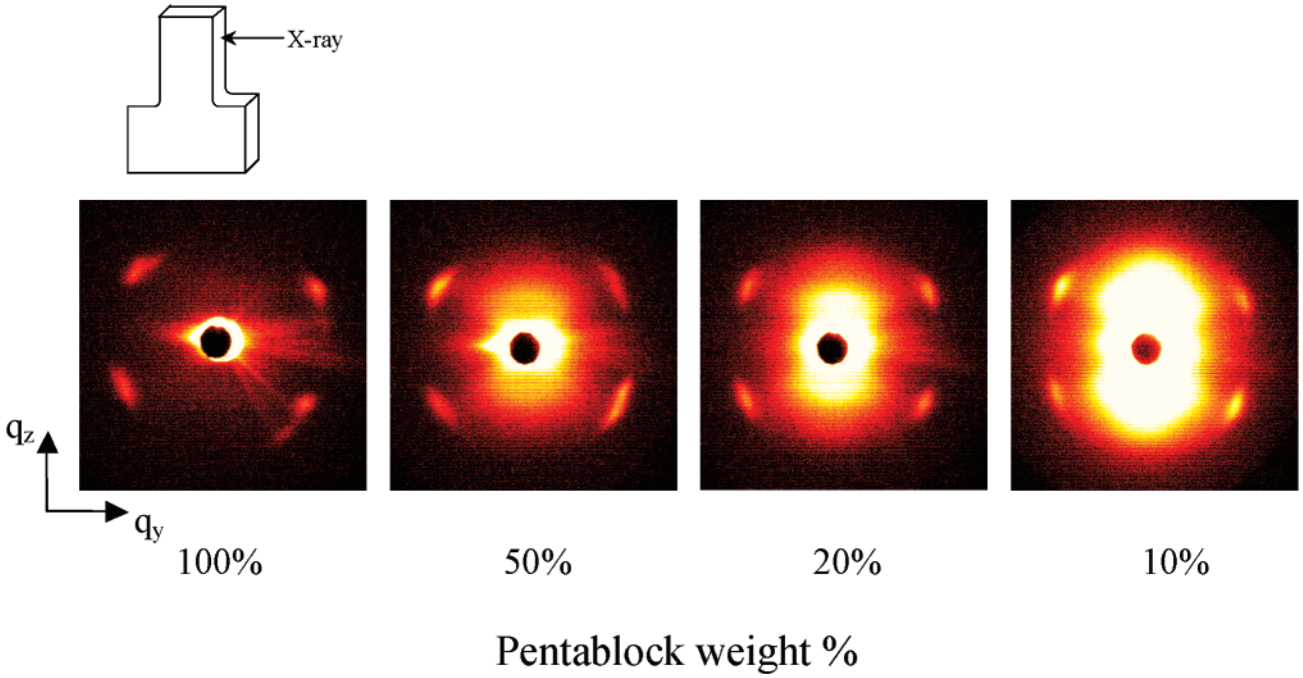

Figure 14. SAXS patterns obtained from fractured tensile specimens with the X-ray beam directed along the width of the stain-whitened material as shown in the sketch. The four-point pattern in each panel is consistent with a lamellae buckling mechanism[24] while the increase in forward scattering intensity with decreasing pentablock content correlates with strain whitening (see Figure 13).

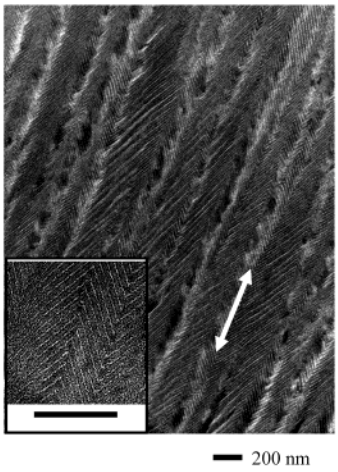

Figure 15. Transmission electron micrograph obtained from the gauge section of the failed 100% CECEC tensile specimen shown in Figure 13. This thin section was stained with ruthenium tetraoxide rendering the C domains dark gray and the E domains nearly white. Bands of tilted lamellae arrange at an angle of about 66° are consistent with the four-spot SAXS pattern found in Figure 14. The viewing angle for this micrograph is coincident with the X-ray beam direction sketched in Figure 14, and the white arrow identifies the strain axis.

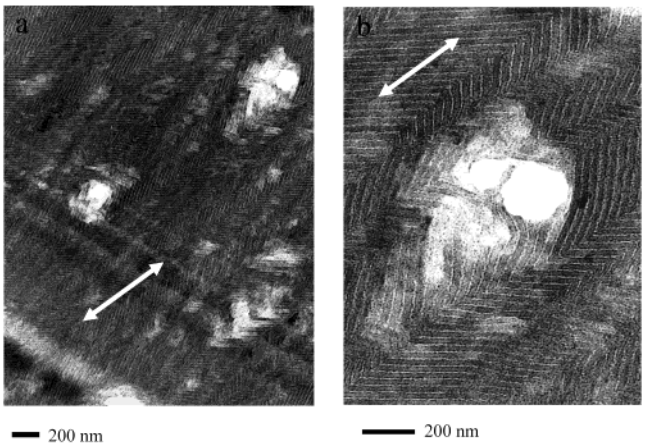

Figure 16. TEM images obtained from the gauge section of the 10% CECEC in CEC tensile specimen. Staining and section orientation are as described in Figure 15. Strain whitening, evident in the photograph of this specimen shown in Figure 13, can be attributed to the formation of voids during necking and drawing. Also evident in these images are the same type of chevron structures present in the void free pure pentablock (see Figure 15). The white arrows indicate the strain axis.

poly(2-vinylpyridine) reinforced with poly(styrene-*b*-2-vinylpyridine) diblock copolymer. They estimated the force required to break a single polymer chain, F, to be about 2×10^{-9} N. The strength of purely bridged lamellae, $\sigma_{bridging}$, can thus be calculated as

$$\sigma_{bridging} = \frac{F}{A} = \frac{2 \times 10^{-9}\,(\mathrm{N})}{2.0 \times 10^{-18}\,(\mathrm{m}^2)} = 1.0 \times 10^{9}\,(\mathrm{Pa}) \quad (3)$$

On the basis of the criterion $\sigma > \sigma_Y$, and ignoring contributions from looping chains, the fraction of uniformly distributed bridging chains required to ensure ductility is simply

$$\frac{C_{bridge}}{C_{total}} = \frac{\sigma_Y}{\sigma_{bridging}} = \frac{30 \times 10^{6}}{1.0 \times 10^{9}} = 0.03 \quad (4)$$

Since each CECEC pentablock has two loose and mechanically ineffective C end blocks, the minimum weight fraction of CECEC pentablock is 3 times this value or 9%, which coincides with the transition region found in Figure 12.

This simple calculation incorporates several gross assumptions. We presume that the applied load is uniformly distributed across all lamellae and neglect

any fluctuations in the degree of alignment and the possibility of defects. And we ignore the role of stress concentration due to bulk defects or surface imperfections. Moreover, this simple calculation deals only with glassy failure.

Before delving into the blend results, we must address an apparent inconsistency between the current and previously reported behavior of the CECEC material. Although the overall stress−strain behavior and four-spot SAXS patterns reported by Hermel et al.[6] for shear-aligned CECEC pentablock copolymer (the same lot of polymer) closely resemble those found in Figures 11a and 14, significantly more strain whitening and much more low-q SAXS intensity were found in our previous investigation. Only one experimental factor differed between these studies. Whereas Hermel et al.[6] employed a shear rate of $\dot{\gamma} = 0.16\ s^{-1}$, here we opted to use $\dot{\gamma} = 0.48\ s^{-1}$ in preparing all the shear-aligned specimens subjected to mechanical testing. Everything else was kept the same, including the thermal history and strain amplitude employed during melt processing and the tensile specimen dimensions and deformation conditions employed during mechanical testing.

Increasing the shear rate probably leads to a more perfect state of lamellae alignment, perhaps eliminating defects that are left by the lower processing rate. To our knowledge this topic has not been addressed with pentablocks. Such defects likely would precipitate damage during plastic deformation, which would produce additional strain whitening and excess low-angle X-ray scattering.

A second plausible explanation relies on shear-induced bridging configurations. In an earlier publication dealing with a different CECEC specimen, Vigild et al.[8] speculated that high rates of reciprocating shear-induce stretched (bridging) chain configurations. As detailed elsewhere,[11] the processing conditions employed here and earlier[6] lie at the transition between the low (domain dominated) and high (single chain dominated) frequency regimes. Tripling the shear rate may have induced a more uniform distribution of bridging configurations, resulting in less permanent damage in the strained pentablock specimens. This effect is worthy of additional research.

The blend results described here must be considered in the context of the pentablock failure model proposed in the previous communication,[6] where we speculated that E domain cavitation followed by lamellae buckling governs necking and strain hardening in CECEC. After buckling the lamellae period returns to its original value, although rotated by about 66°, which accounts for the four-spot SAXS pattern. We believe domain stitching is responsible for this elastic rebound; anchoring of softer E blocks in glassy C domains, toughened by bridging blocks, permits nearly full elastic recovery of the cavitated semicrystalline lamellae. Here we must emphasize that this model has not been proven.

Adding CEC triblock copolymer diminishes the percentage of bridging C blocks, which is likely to weaken the material. Cavitation within the E domains may be accompanied by more pullout of C end blocks, a process that probably is irreversible. Residual strain whitening and forward scattering of X-rays in the failed specimens are consistent with this hypothesis. We suggest that such pullout produces permanent damage, which reduces the strain at break and ultimately leads to brittle failure when the fraction of pentablock reaches 10−15%. Remarkably the four-spot patterns appear to be unaffected by these events, implying that macroscopic buckling is not impeded by or correlated with these microscopic processes. We believe this also is consistent with our model: initial cavitation of the E domains leading to unstable lamellae that buckle. Prior to buckling both systems behave similarly. However, after buckling the pure pentablock can recover while chain pullout leaves permanent voids in the blends. The TEM pictures presented in Figures 15 and 16 support this interpretation. Lamellae chevron formation is apparent in both the CECEC and 10% CECEC systems with strain-induced cavitation verified in the latter.

Finally, although there is no direct or obvious connection between the transition in melt flow behavior at 10−15% pentablock (Figure 10) and the transition from brittle to ductile behavior in the solid state at 5−15% pentablock (Figure 12), we do not believe this correspondence is a coincidence. We suspect that the mechanism responsible for the perpendicular lamellae orientation involves chain extension (stretching), which also maximizes bridging configurations. Although far from conclusive, our calculation for theoretical strength, which assumes complete bridging, and the discussion of the blend failure behavior lend support to the notion that shear alignment of multiblock copolymers is accompanied by significant conformational rearrangements.

Conclusions

This study has explored relationships between molecular architecture and two types of deformation in lamellae-forming block copolymers blends: melt state reciprocating shear and solid-state tensile deformation. Blending CECEC pentablock with CEC triblock resulted in significant modifications to both classes of physical properties. Just 10−15 wt % CECEC pentablock copolymer in triblock/pentablock blends is sufficient to induce pentablock-like characteristics, including a perpendicular lamellae alignment at strain amplitudes $0.5 \leq \gamma \leq 5$ and a ductile response under tensile deformation. We attribute these properties to molecular stretching during shear alignment and domain bridging of the center C blocks, which provides strength to the otherwise brittle glassy domains in the solid state. Addition of CEC to CECEC results in strain whitening and a reduction in strain to break due to void formation during yielding and necking.

This type of molecular reinforcement is reminiscent of the concept of a molecular composite, popularized as an ideal way to enhance the mechanical properties of brittle materials.[48] A homogeneous polymer blend containing rigid-rod-like and amorphous polymers can be termed a “molecular composite” since the rodlike polymer acts as a reinforcing filler dispersed within an amorphous matrix at a molecular scale. However, rodlike polymers are notoriously incompatible with other polymers due to a lack of mixing entropy, obviating the ability to form homogeneous molecular composites. In this study, multiblock copolymers (CECEC) were guided to self-assembly into an otherwise brittle lamellar material (CEC) with mechanically reinforcing stretched configurations, resulting in improvements in toughness in much the same way that molecular composites are supposed to behave.

This work establishes pentablock/triblock blending as a viable approach to manipulate the degree of domain

"stitching" in ordered glassy/semicrystalline systems. Resolution of the detailed microscopic mechanisms responsible for the macroscopic properties reported here will require additional experimentation using TEM, SAXS, and perhaps light and neutron scattering. This work will be undertaken in the near future.

Acknowledgment. This study was supported by the U.S. Department of Energy under Contract DEAC05-960R22464. Additional support was provided by the Medtronic Corp. Theresa J. Hermel is thanked for many helpful conversations and assistance with the experimental techniques. Stephen F. Hahn kindly provided well-characterized materials for this study for which we are grateful.

References and Notes

(1) Holden, G.; Legge, N. R.; Quirk, R. P.; Schroeder, H. E. *Thermoplastic Elastomers*, 2nd ed.; 1996.
(2) Fredrickson, G. H.; Bates, F. S. *Annu. Rev. Mater. Sci.* **1996**, *26*, 501.
(3) Bates, F. S.; Rosedale, J. H.; Bair, H. E.; Russell, T. P. *Macromolecules* **1989**, *22*, 2557.
(4) Bates, F. S.; Fredrickson, G. H.; Hucul, D. A.; Hahn, S. F. *AIChE J.* **2001**, *47*, 762.
(5) Hucul, D. A.; Hahn, S. F. *Adv. Mater.* **2000**, *12*, 1855.
(6) Hermel, T. J.; Hahn, S. F.; Chaffin, K. A.; Gerberich, W. W.; Bates, F. S. *Macromolecules* **2003**, *36*, 2190.
(7) Hermel, T. J.; Wu, L.; Hahn, S. F.; Lodge, T. P.; Bates, F. S. *Macromolecules* **2002**, *35*, 4685.
(8) Vigild, M. E.; Chu, C.; Sugiyama, M.; Chaffin, K. A.; Bates, F. S *Macromolecules* **2001**, *34*, 951.
(9) Watanabe, H. *Macromolecules* **1995**, *28*, 5006.
(10) Hamley, I. W. *J. Phys.: Condens. Matter* **2001**, *13*, 643.
(11) Chen, Z. R.; Kornfield, J. A.; Smith, S. D.; Grothaus, J. T.; Satkowski, M. M. *Science* **1997**, *277*, 1248.
(12) Chen, Z. R.; Kornfield, J. A. *Polymer* **1998**, *19*, 4679.
(13) Koppi, K. A.; Tirrell, M.; Bates, F. S.; Almdal, K. *J. Phys. II* **1992**, *2*, 1941.
(14) Koppi, K. A.; Tirrell, M.; Bates, F. S.; Almdal, K. *Phys. Rev. Lett.* **1993**, *70*, 1449.
(15) Koppi, K. A.; Tirrell, M.; Bates, F. S.; Almdal, K.; Mortenesen, K. J. *J. Rheol.* **1994**, *38*, 999.
(16) Tepe, T.; Hajdul, D. A.; Hillmyer, M. A.; Weimann, P. A.; Tirrell, M.; Bates, F. S.; Almdal, K.; Mortenesen, K. J. *J. Rheol.* **1997**, *41*, 1147.
(17) Gupta, V. K.; Krishnamoorti, R.; Kornfield, J. A.; Smith, S. D. *Macromolecules* **1996**, *29*, 1359.
(18) Gupta, V. K.; Krishnamoorti, R.; Chen, Z. R.; Kornfield, J. A.; Smith, S. D.; Satowski, M. M.; Grothaus, J. T. *Macromolecules* **1996**, *29*, 875.
(19) Gupta, V. K.; Krishnamoorti, R.; Kornfield, J. A.; Smith, S. D. *Macromolecules* **1995**, *28*, 4464.
(20) Winey, K. I.; Patel, S. S.; Larson, R. G.; Watanabe, H. *Macromolecules* **1993**, *26*, 2542.
(21) Patel, S. S.; Winey, K. I.; Larson, R. G.; Watanabe, H. *Macromolecules* **1995**, *28*, 4313.
(22) Weidish, R.; Stamm, M.; Micheler, G. H.; Fischer, H.; Jerome, R. *Macromolecules* **1999**, *32*, 742.
(23) Weidish, R.; Schreyeck, G.; Ensslen, M.; Micheler, G. H.; Stamm, M.; Scubert, D. W.; Budde, H.; Horing, S.; Arnold, M.; Jerome, R. *Macromolecules* **2000**, *33*, 5495.
(24) Kawai, H.; Hashimoto, T.; Miyoshi, K.; Uno, H.; Fujimura, M. *J. Macromol. Sci., Phys.* **1980**, *B17*, 427.
(25) Cohen, Y.; Albalak, R. J.; Dair, B. J.; Capel, M. S.; Thomas, E. L. *Macromolecules* **2000**, *33*, 6502.
(26) Cohen, Y.; Brinkman, M.; Thomas, E. L. *J. Chem. Phys.* **2001**, *114*, 984.
(27) Seguela, R.; Prud'homme, J. *Macromolecules* **1981**, *14*, 197.
(28) Sakurai, S.; Sakamoto, J.; Shibayama, M.; Nomura, S. *Macromolecules* **1993**, *26*, 3351.
(29) Pakula, T.; Saijo, K.; Kawai, H.; Hashomoto, T. *Macromolecules* **1985**, *18*, 1294.
(30) Yu, J. M.; Dubois, P.; Jerome, R. *Macromolecules* **1996**, *29*, 8362.
(31) Yamaoka, I.; Kimura, M. *Polymer* **1993**, *34*, 4399.
(32) Ruokolainen, J.; Fredickson, G. H.; Kramer, E. J.; Ryu, C. Y.; Hahn, S. H.; Magonov, S. N. *Macromolecules* **2002**, *35*, 9391.
(33) Dair, B. J.; Honeker, C. C.; Alward, D. B.; Avgeropoulos, A.; Hadjichristidis, N.; Fetters, L. J.; Capel, M.; Thomas, E. L. *Macromolecules* **1999**, *32*, 8145.
(34) Ryu, C. Y.; Ruokolainen, J.; Fredickson, G. H.; Kramer, E. J.; Hahn, S. H. *Macromolecules* **2002**, *35*, 2157.
(35) Hermel, T. J. Ph.D. Thesis, University of Minnesota, Minneapolis, 2003.
(36) Zhao, J.; Hahn, S. F.; Hucul, D. A.; Meunier, D. M. *Macromolecules* **2001**, *34*, 1737.
(37) Zhao, J.; Majumdar, B.; Schulz, M. F.; Bates, F. S.; Almdal, K.; Mortensen, K.; Hajduk, D. A.; Gruner, S. M. *Macromolecules* **1996**, *29*, 1204.
(38) Rosedale, J. H.; Bates, F. S. *Macromolecules* **1990**, *23*, 2329.
(39) Gehlsen, M. D.; Almdal, K.; Bates, F. S *Macromolecules* **1992**, *25*, 939.
(40) Bates, F. S.; Rosedale, J. H.; Fredickson, G. H. *J. Chem. Phys.* **1990**, *92*, 6255.
(41) Koppi, K. A. Ph.D. Thesis, University of Minnesota, Minneapolis, 1993.
(42) ASTM, D638-95, *Standard Test Method for Tensile Properties of Plastics*, in Annual Book of ASTM Standards. 1996; ASTM.45.
(43) Fredrickson, G. H.; Helfand, E. J. *J. Chem. Phys.* **1987**, *87*, 697.
(44) Almdal, K.; Bates, F. S.; Mortensen, K. J. *J. Chem. Phys.* **1992**, *96*, 9122.
(45) Cochran, E. W.; Bates, F. S *Macromolecules* **2002**, *35*, 7368.
(46) Cochran, E. W.; Morse, D. C.; Bates, F. S. *Macromolecules* **2003**, *36*, 782.
(47) Creton, C.; Kramer, E. J.; Hui, C. Y.; Brown, H. R. *Macromolecules* **1992**, *25*, 3075.
(48) Viswanathan, S.; Dadmun, M. D. *Macromolecules* **2002**, *35*, 5049.

MA035300Q